ACS APPLIED MATERIALS & INTERFACES

Research Article

www.acsami.org

Effect of SiO_2 Spacer-Layer Thickness on Localized Surface Plasmon-Enhanced ZnO Nanorod Array LEDs

Weizhen Liu,[†,‡] Haiyang Xu,[*,†] Siyi Yan,[†] Cen Zhang,[†] Lingling Wang,[†] Chunliang Wang,[†] Liu Yang,[†] Xinhua Wang,[‡] Lixia Zhang,[§] Jiannong Wang,[§] and Yichun Liu[*,†]

[†]Centre for Advanced Optoelectronic Functional Materials Research and Key Laboratory for UV Light-Emitting Materials and Technology of Ministry of Education, Northeast Normal University, Changchun 130024, China

[‡]State Key Laboratory of Applied Optics, Changchun Institute of Optics, Fine Mechanics and Physics, Chinese Academy of Sciences, Changchun 130033, China

[§]Department of Physics, Hong Kong University of Science and Technology, Clear Water Bay, Kowloon, Hong Kong

Supporting Information

ABSTRACT: Localized surface plasmon (LSP)-enhanced ultraviolet LEDs have been constructed via spin-coating Ag nanoparticles onto ZnO/SiO_2 core/shell nanorod array/p-GaN heterostructures. Different from the previous reports where the dielectric spacer-layer thickness was determined only through photoluminescence (PL) characterization, the SiO_2 shell thickness in this work is also optimized by actual electroluminescence (EL) measurements to maximize the enhancement. It is interesting to find that the enhancement ratios derived from PL and EL measurements demonstrate different thickness dependences on SiO_2 shell: an optimal 3.5-fold PL enhancement was obtained at the SiO_2 thickness of 16 nm, while an "abnormal" 7-fold EL enhancement was achieved at the thickness of 12 nm. Time-resolved spectroscopy studies, as well as theoretical estimations and numerical simulations, reveal that the higher-ratio EL enhancement stems from joint contributions, both internal-quantum-efficiency improvement induced by exciton-LSP coupling and light-extraction-efficiency improvement aroused by photon-LSP coupling.

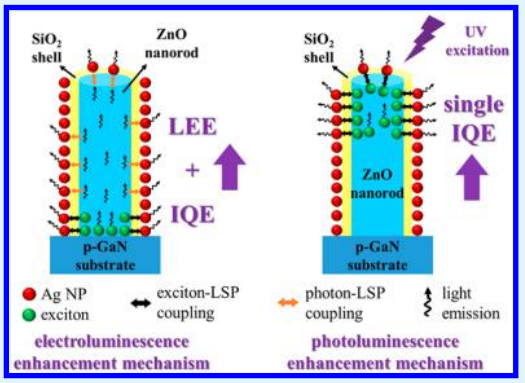

KEYWORDS: *localized surface plasmon, ZnO/SiO_2 core/shell nanorod array, ultraviolet LED, luminescence enhancement, exciton-LSP coupling, photon-LSP coupling*

1. INTRODUCTION

ZnO is regarded as a promising candidate for ultraviolet (UV) LEDs and low-threshold laser diodes due to its wide direct band gap (3.37 eV) and large exciton binding energy (60 meV).[1−8] However, the electroluminescence (EL) efficiency of ZnO-based LEDs on either homojunctions or heterojunctions is not as high as expected due to the poor quality of p-type ZnO or considerable amounts of heterointerface defects. To improve the efficiency, two approaches have been proposed and proved effective. One is employing one-dimensional single-crystalline ZnO nanowires/nanorods as the active layers for LEDs, since a remarkable increase of carrier injection rate has been observed in these nanosized light emitters.[3−6] The other is introducing metal localized surface plasmons (LSPs) into the LED design. The resonant coupling between semiconductor excitons/photons and metal LSPs enables the creation of additional recombination/extraction paths, improving both the internal-quantum-efficiency (IQE) and light-extraction-efficiency (LEE) of the LEDs.[9−18]

The thickness of dielectric spacer-layer between metal and ZnO plays a very important role in improving the luminescence efficiency of LSPs decorated ZnO-based materials and devices.[6,19−25] Thus, many groups optimized the spacer-layer thickness through photoluminescence (PL) measurements in consideration of suppressing undesired charge transfer and nonradiative Förster resonant energy transfer (FRET) between metal and ZnO.[19−25] For example, Mahanti et al. have studied the effect of SiO_2 spacer-layer thickness on the PL enhancements of Au and Ag nanoparticles (NPs) decorated ZnO nanorod arrays (NRAs) in detail.[24,25] The PL optimized spacer-layer thickness was directly employed for the subsequent LED fabrication and obtained a so-called "LSP-induced EL enhancement". However, the so-called "optimal" thickness derived only from PL characterizations cannot be directly adopted for EL operation, because spacer-layer will also act as potential barrier layer and seriously affect the carrier injection and transportation properties under external bias. This point is very crucial to LSP-induced EL enhancement, which must be carefully studied in actual EL process. Thus, to obtain the most suitable spacer-

Received: September 7, 2015
Accepted: January 7, 2016
Published: January 7, 2016

DOI: 10.1021/acsami.5b08382
ACS Appl. Mater. Interfaces 2016, 8, 1653−1660

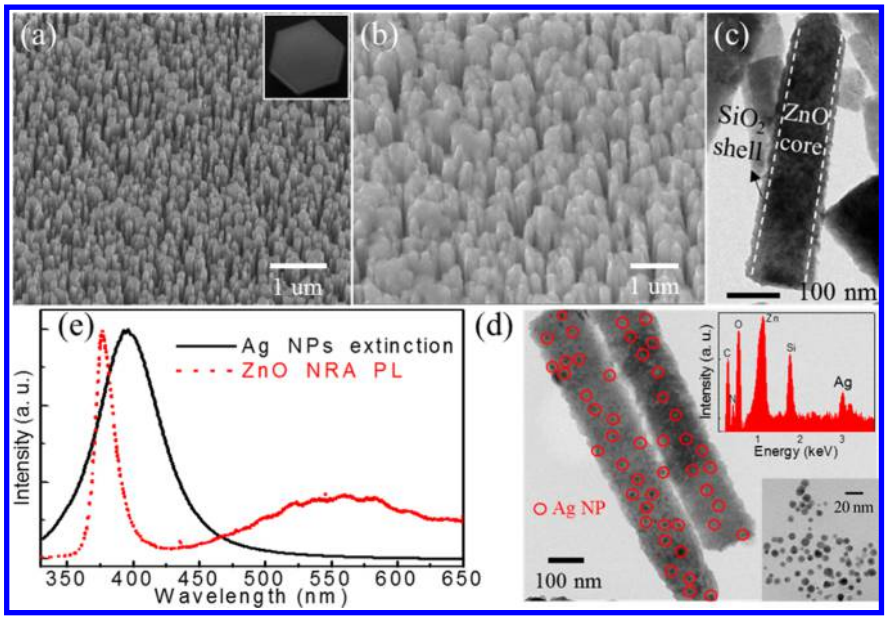

Figure 1. (a and b) Tilted-view SEM images of a bare ZnO NRA and a ZnO/SiO_2 core/shell NRA; (inset a) hexagonal end face of an as-grown ZnO nanorod. (c) A typical TEM image of a ZnO/SiO_2 core/shell nanorod with shell layer of 16 nm; the white dashed lines are drawn as guide lines to clarify the core/shell heterostructure. (d) A typical TEM image of ZnO/SiO_2 core/shell nanorods with Ag NPs decoration; (insets) are the energy dispersive X-ray spectrum of Ag coated core/shell nanorods (upper right) and a TEM image of Ag NPs distributed on a TEM grid with carbon membrane (bottom right). (e) The LSP resonant extinction spectrum of Ag NPs (black solid line) and a typical PL spectrum of ZnO NRA (red dot line).

layer thickness for LSP-enhanced LED, thickness optimization via actual EL measurements is required and more meaningful.

In this work, LSP-enhanced ZnO NRA UV LEDs were fabricated by spin-coating Ag NPs onto ZnO/SiO_2 core/shell NRA/p-GaN heterostructures. For the first time, the thicknesses of SiO_2 shell layers (also as spacer-layers) were optimized through both PL measurements and in situ EL characterizations. It is interesting to find that the optimal enhancement ratios derived from PL and EL characterizations show distinctively different thickness dependences on SiO_2 shell. To figure out this "tricky" phenomenon, time-resolved luminescence measurements and theoretical estimations, as well as finite-difference time-domain (FDTD) numerical simulations were carried out and studied in detail. To our best knowledge, there have been no reports yet to optimize the spacer-layer thickness based on the actual EL method.

2. EXPERIMENTAL SECTION

The ZnO NRAs were epitaxially grown on the commercially available p-GaN:Mg/Al_2O_3 (0001) substrates (hole concentration, 3.44×10^{17} cm^{-3}; Hall mobility, 10.2 $cm^2/(V\ s)$; rectangle size, 5 × 6 mm) by a simple hydrothermal synthesis using zinc acetate and hexamethylenetetramine as precursors.[26] Then, SiO_2 shell layers were coated onto the as-grown ZnO NRAs by a layer-by-layer (LbL) deposition method.[27,28] Different from traditional physical deposition techniques (e.g., pulsed laser deposition and magnetron sputtering) which always suffer from the problem of nonuniform coating due to the shadow effect, the LbL deposition employed here allows uniform coating and easy control of shell layer thickness. According to our previous work, the average coating rate of SiO_2 shell onto ZnO nanorod for LbL deposition is 4 nm/cycle.[27] Thus, the silica shell thickness can be flexibly modulated via a multicycle LbL deposition strategy. More experimental details for the preparation of ZnO/SiO_2 core/shell NRAs are described in the Supporting Information, Figure S1. Afterward, Ag NPs colloidal solutions (Sigma-Aldrich, 0.02 mg/mL, containing sodium citrate as stabilizer) were spin-coated (rotation speed: 2000 r/min) onto these as-prepared ZnO/SiO_2 core/shell NRAs. X-ray diffraction (XRD) patterns of these core/shell NRAs with and without Ag NPs decoration are shown in the Supporting Information, Figure S2, which confirm the good crystallinity of synthesized ZnO/SiO_2 core/shell NRAs. To construct heterojunction LEDs, metals Au/Ni and In circular pads are selected as the contact electrodes for p-GaN:Mg substrates and n-ZnO NRAs, respectively, and the electrode's diameter is around 1 mm. The EL signal output is collected from the surrounding area of the top metal In electrode, and all spectra (including PL and EL) were measured and collected at the same experimental conditions in order to allow comparison.

3. RESULTS AND DISCUSSION

Figure 1a shows the scanning electron microscopy (SEM) image of an as-grown bare ZnO NRA. It can be seen that they are highly ordered and are vertically aligned on p-GaN substrates. The mean size of the bare ZnO nanorods is 120 nm in diameter and 1 um in length. Through the multicycle LbL deposition of SiO_2 shell layer, the composite NRAs with clear core/shell heterostructures were obtained, and their typical SEM and transmission electron microscopy (TEM) images are shown in Figure 1b,c. After the succeeding spin-coating process, Ag NPs with mean size of 10 nm were distributed throughout the core/shell nanorods' surface, and the Ag NPs decorated ZnO/SiO_2 core/shell nanorods have been formed (Figure 1d and insets). As mentioned above, the SiO_2 shell introduced here acts as spacer-layer between ZnO nanorods and Ag NPs. Therefore, their thicknesses should be controlled within a proper range. According to previous reports, the penetration depth (Z) of the Ag LSP evanescent field into SiO_2 is given by $Z = \lambda/2\pi\sqrt{(\varepsilon'_d - \varepsilon'_m)/\varepsilon'^2_d}$, where ε'_d and ε'_m are the real part of the dielectric constants of SiO_2 and Ag, and λ is the wavelength of incident light.[9,15] At near UV region, the permittivity of SiO_2 is in the range of 3.0 to 5.0, while that of Ag is around −2.8.[4,15] The calculations reveal that Z values between 33 and 49 nm for the ZnO UV emission

DOI: 10.1021/acsami.5b08382
ACS Appl. Mater. Interfaces 2016, 8, 1653−1660

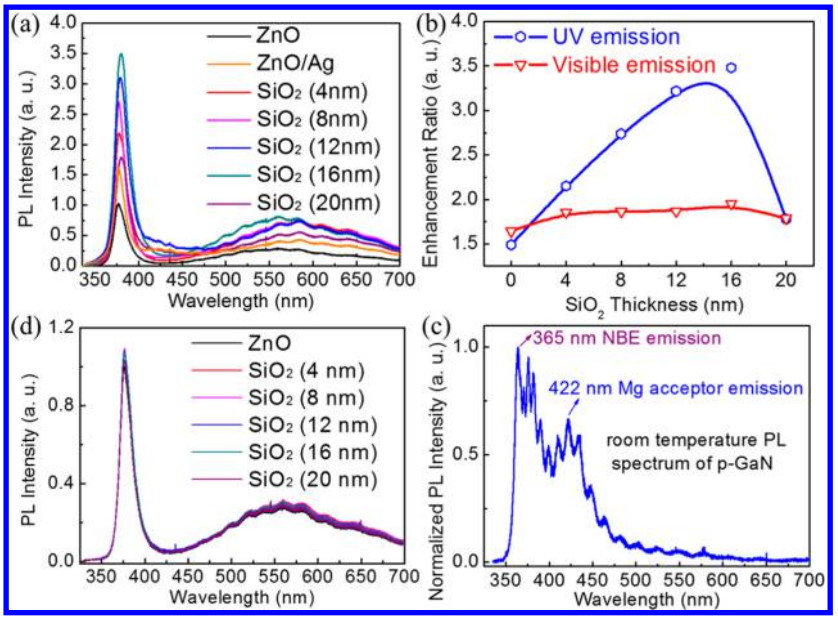

Figure 2. (a) RT PL spectra of bare ZnO NRA and Ag NPs decorated ZnO/SiO_2 core/shell NRAs with different SiO_2 layer thicknesses. (b) The variations of enhancement ratios of integrated UV (blue hexagon) and visible (red triangle) emission intensity with the SiO_2 spacer-layer thickness. (c) PL spectra of the bare p-GaN substrate. (d) PL spectra of bare ZnO NRA and NRAs only coated with different SiO_2 shell layer thicknesses (without Ag NPs decoration).

wavelength of 380 nm. To ensure the occurrence of resonant coupling between ZnO excitons and Ag LSPs, SiO_2 shell thickness should be controlled within 30 nm in our experiments. Herein, SiO_2 spacer-layers with different thicknesses ranging from 0 to 20 nm were inserted between Ag NPs and ZnO nanorods to find the maximum luminescence enhancement, and this will be discussed in detail in Figures 2 and 5. Figure 1e gives the LSP resonance extinction spectrum of the Ag NPs used here, which is centered at a wavelength of 395 nm. The relatively broad distribution of this extinction band may result from the size fluctuation of Ag NPs and the coupling between neighboring LSPs.[13,29] An obvious spectral overlap is observed between the ZnO UV luminescence and Ag LSP resonance extinction, suggesting the possibility of a resonant coupling between ZnO excitons/photons and Ag LSPs. Thus, the enhanced UV emission from ZnO/SiO_2 core/shell NRAs would be expected.

Figure 2a presents the room temperature (RT) PL spectra of bare ZnO NRA and Ag NPs decorated ZnO/SiO_2 NRAs with different shell layer thicknesses. It is known that the LSP-enhanced PL is usually attributed to two independent processes: excitation (absorption) enhancement or emission enhancement.[8,14] In our PL measurements, a 325 nm line of a He−Cd laser was used as the excitation source, which is far away from the LSP resonance wavelength of 395 nm, thus excluding the excitation enhancement effect. In Figure 2(a), one can see that all spectra consist of a near-band-edge (NBE) emission peak at 380 nm and a relatively weak and broad deep-level (DL) emission band centered at 560 nm.[30] Herein, the DL emission band is very likely induced by the surface defects of synthesized ZnO nanorods (e.g., oxygen vacancies) due to the relatively large aspect ratio of the nanorods.[14,25] The ZnO UV PL is enhanced even though the Ag NPs are directly coated onto the bare ZnO NRA. As mentioned earlier, the introduction of SiO_2 spacer-layer can suppress the undesired charge transfer and nonradiative FRET processes, thus resulting in further PL improvement. With increasing SiO_2 shell layer thickness, the ZnO UV emission gradually increases. A maximum ~3.5-fold enhancement of the integrated UV emission intensity is obtained when the SiO_2 thickness reaches 16 nm. Further increase in shell layer thickness only leads to the reduction of PL enhancement due to the evanescent wave nature of LSP resonant field. Such a variation trend is also illustrated in Figure 2b. In contrast, only very weak enhancement ratios ranging between 1.5 and 2.0 are observed in the visible emission region, probably due to the much less spectral overlap between ZnO DL emission and Ag LSP resonance extinction. In addition, the RT PL spectra of bare p-GaN substrate and ZnO NRAs coated only with different SiO_2 thicknesses (without Ag NPs decoration) are also given in Figures 2c,d, respectively. As can be seen, the spectrum of bare p-GaN substrate is composed of two broad emission bands peaked at 365 (the NBE emission) and 422 nm (Mg acceptor-related emission), which is noticeably different from the PL spectra of ZnO NRAs. Hence, the observed UV emission and relevant PL enhancement phenomena are just from the ZnO/SiO_2 core/shell NRAs. As to the spectra of ZnO NRAs coated only with different SiO_2 thicknesses in Figure 2d, they look almost the same with a negligible enhancement ratio (<1.1-fold) after SiO_2 coating. Thus, the surface modification of SiO_2 coatings does not play an efficient role in the observed UV emission enhancements.

To confirm that the luminescence enhancements indeed originate from the resonant couplings between Ag LSPs and ZnO excitons, we performed RT time-resolved PL (TR-PL) measurements by employing a streak camera (temporal resolution: 2 ps), and a femtosecond pulsed laser (wavelength, 266 nm; repetition rate, 76 MHz; pulse width, 200 fs) as signal detector and excitation source, respectively. Figure 3 shows the TR-PL spectra of the bare ZnO NRA and ZnO/SiO_2 core/shell NRAs (with 16 nm SiO_2) with and without Ag NPs decoration, respectively; the monitoring wavelength was fixed at 380 nm. As can be seen, the three samples exhibit distinctly different fluorescence decay rates, and corresponding decay curves can

DOI: 10.1021/acsami.5b08382
ACS Appl. Mater. Interfaces 2016, 8, 1653−1660

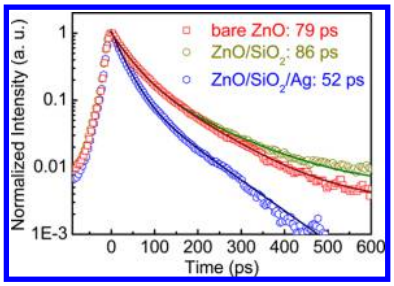

Figure 3. RT TR-PL spectra of bare ZnO NRA (red square) and ZnO/SiO_2 core/shell NRAs with (blue hexagon) and without (dark yellow circle) Ag NPs; the thickness of silica shell is 16 nm and the solid lines are the fits to a biexponential decay model.

be well fitted by a biexponential attenuation function. Through a weighted average of two time constants, the effective UV fluorescence lifetimes for the bare ZnO NRA, ZnO/SiO_2 core/shell NRA and Ag NPs decorated core/shell NRA are determined to be 79, 86, and 52 ps, respectively. Generally speaking, excitons in semiconductor decay via both radiative and nonradiative recombination channels. Thus, the PL lifetime for bare ZnO NRA (τ) can be expressed as[9]

$$\frac{1}{\tau} = k_{rad} + k_{non} \tag{1}$$

where the k_{rad} and k_{non} represent the radiative and nonradiative recombination rates of ZnO nanorods, respectively. After the SiO_2 shells were coated onto the nanorods' surface, the surface defects/traps were passivated in some extent, leading to the reduction of k_{non}.[31] Therefore, the SiO_2 coating results in a slight increase of ZnO fluorescence lifetime. However, by further introducing Ag NPs into the core/shell NRAs, an additional decay channel, exciton-LSP interaction, should be taken into account, and the PL lifetime for Ag NPs decorated core/shell NRA (τ^*) is written as[8,9]

$$\frac{1}{\tau^*} = k_{rad} + k_{non} + k_{sp} \tag{2}$$

here, the k_{sp} is the exciton-LSP coupling rate and is believed to be much faster than the k_{rad} and k_{non}. Hence, the spontaneous radiation rate of Ag NPs decorated core/shell NRA is increased, resulting in a decrement of observed PL lifetime. That is, the shortened PL lifetime indicates that the LSP provides an additional, high-rate recombination channel, and is regarded as a strong evidence for exciton-LSP coupling.

Usually, the increase in recombination rate will also induce the improvement of IQE. In theory, the IQE for the samples with and without Ag NPs (η^*_{IQE} and η_{IQE}) can be written as[9]

$$\eta_{IQE} = \frac{k_{rad}}{k_{rad} + k_{non}} \tag{3}$$

and

$$\eta^*_{IQE} = \frac{k_{rad} + C'_{ext}k_{sp}}{k_{rad} + k_{non} + k_{sp}} \tag{4}$$

where the C'_{ext} is the probability of photon extraction from the LSP's energy and is generally assumed close to 100%.[11] From the eqs 3 and 4, it is easy to deduce that the η^*_{IQE} can be improved compared with the η_{IQE} because of $\eta^*_{IQE} - \eta_{IQE} = ((k_{non} \times k_{sp})/((k_{rad} + k_{non} + k_{sp}) \times (k_{rad} + k_{non}))) > 0$. Combining eqs 1−4, the IQE ratio between Ag LSPs decorated NRA and bare ZnO NRA can be expressed as[13]

$$\frac{\eta^*_{IQE}}{\eta_{IQE}} = \frac{\eta_{IQE} + C'_{ext}(F_p - 1)}{F_p\eta_{IQE}} \tag{5}$$

where the $F_p = \tau/\tau^*$ is a Purcell enhancement factor ($F_p = 1.52$ in this work), which depicts the increase in spontaneous recombination rate.[31,32] According to our previous findings, the η_{IQE} for ZnO nanostructures estimated from temperature-dependent PL spectra is around 12%.[8] A rough estimate, based on eq 5, shows that the η^*_{IQE} is 3.5 times as large as η_{IQE}, which is in good agreement with the optimal 3.5-fold PL enhancement ratio, as shown in Figure 2. This "coincidence" reflects that the PL enhancement observed here is mainly attributed to the IQE improvement induced by exciton-LSP coupling.

Figures 4a,b exhibit the structural schematic diagram and current−voltage (I−V) curves of our LSP-enhanced NRA LEDs with different SiO_2 thicknesses, respectively. Good ohmic contacts have been formed between Au/Ni electrodes and p-GaN:Mg substrates, as confirmed by a linear I−V relationship in the inset of Figure 4b. Indium pad is supposed to easily form ohmic contact with n-ZnO based materials. It is found that all devices demonstrate typical rectifying diode-like behaviors with obvious asymmetry under the sweeping of applied biases. The turn-on voltage for the bare ZnO NRA/p-GaN heterojunction LED is 5 V. After coating Ag NPs directly onto the bare ZnO NRA's surface, the injection current slightly increases as a result of the formation of more conductive pathways on the nanorod's surface for leakage current.[6,13] However, as the SiO_2 shell layers were inserted between ZnO nanorods and Ag NPs, the injection current gradually decreases with the increasing shell

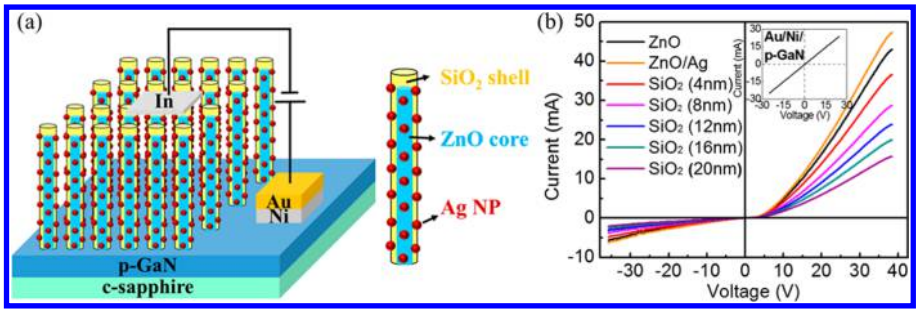

Figure 4. (a) Structural diagram of our LSP-enhanced ZnO/SiO_2 core/shell NRA LED. (b) RT I−V curves of the LSP-enhanced core/shell NRA LEDs with different SiO_2 shell layer thicknesses; the linear I−V characteristic in the inset verifies the good ohmic contact between Au/Ni electrode and p-GaN:Mg substrate.

DOI: 10.1021/acsami.5b08382
ACS Appl. Mater. Interfaces 2016, 8, 1653−1660

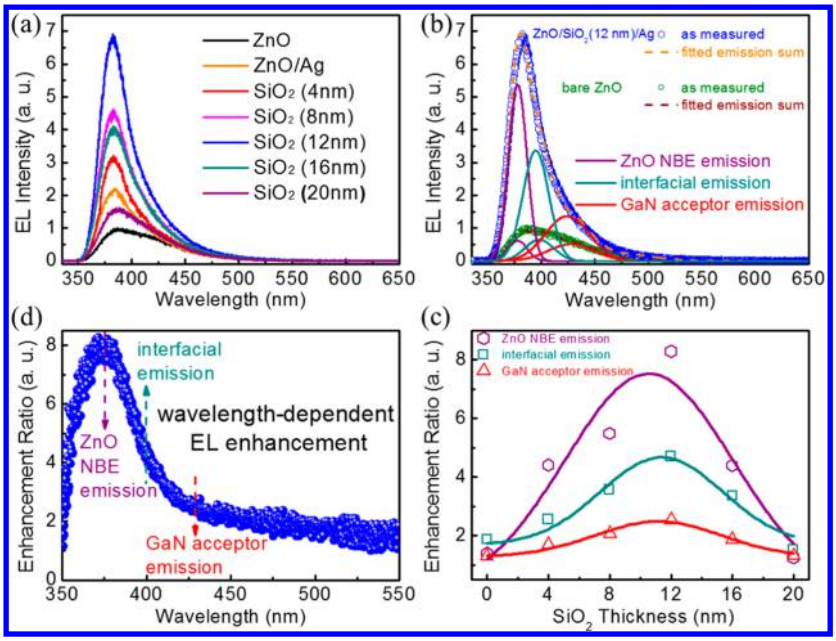

Figure 5. (a) RT EL spectra of bare ZnO NRA and Ag NPs decorated core/shell NRAs with different SiO_2 shell thicknesses; the injection current is fixed at 5 mA. (b) Gaussian deconvolution analyses of the near-UV EL spectra for the bare ZnO NRA LED (olive circle) and Ag NPs decorated core/shell NRA LED (blue hexagon); the shell thickness is 12 nm. (c) The variation of enhancement ratios of three different EL components with SiO_2 shell thicknesses. (d) The dependence of EL enhancement ratio on emission wavelength.

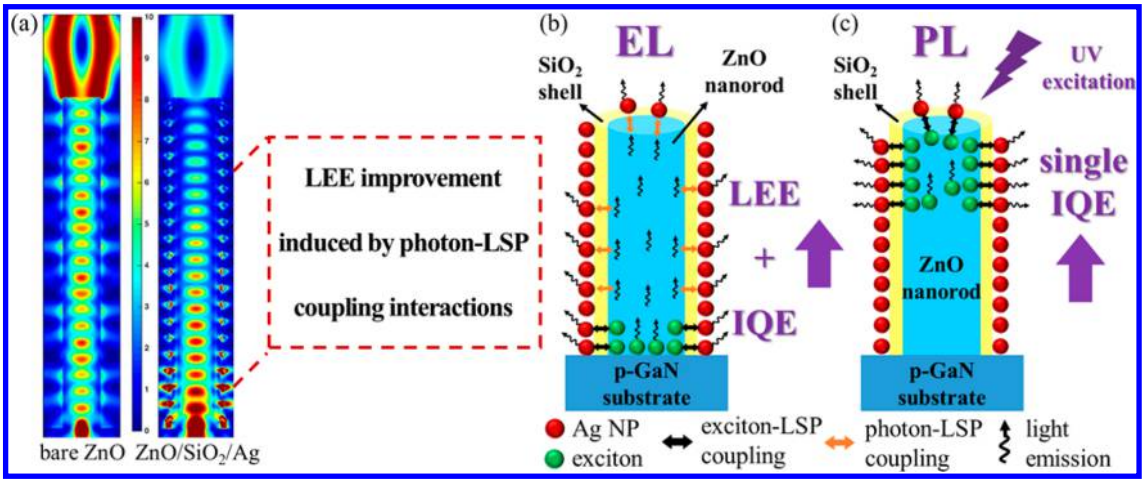

Figure 6. (a) FDTD simulations of the EL propagation behaviors in (left) a bare ZnO nanorod and (right) an Ag NPs decorated core/shell nanorod; the latter clearly shows the LEE improvement induced by photon-LSP coupling interactions. Models illustrating the different enhancement mechanisms in (b) EL (IQE improvement + LEE improvement) and (c) PL (single IQE improvement), respectively.

thickness, which also indicates that the thin dielectric silica coatings indeed play the roles of spacer-layers and can suppress the unwanted charge transfer between metal and semiconductor.

The RT EL spectra of bare ZnO NRA and Ag NPs decorated core/shell NRAs with different shell-layer thicknesses were recorded and plotted in Figure 5a. Under forward bias, all the NRA LEDs show a single near-UV emission band peaked at 384 nm at the same injection current of 5 mA, whereas no detectable EL signal was observed in the visible region. Similar to the case of PL described above, their EL intensity is improved as the Ag NPs and SiO_2 spacer-layer were coated onto the nanorods' surface and a maximum ~7-fold enhancement is obtained at the SiO_2 shell layer thickness of 12 nm. Because this near-UV EL band is relatively broad and is usually believed to be composed of several luminescence components, multipeak deconvolution fittings with Gaussian function (Figure 5b) are helpful to understand the EL enhancement phenomena. It is found that for all LEDs, their broad near-UV emission bands can be well fitted with three individual peaks centered at 378, 397, and 427 nm, which can be ascribed to ZnO NBE excitonic emission, interfacial radiative recombination, and Mg acceptor-related emission of p-GaN, respectively.[2,33] Figure 5c,d displays the detailed enhancement ratios of each EL component and the wavelength-dependent EL enhancement curve (a curve defined by the EL intensity ratio of Ag NPs decorated core/shell NRA LED to the bare ZnO NRA LED; the thickness of SiO_2 shell is 12 nm), respectively. Obviously, the ZnO NBE emission shows the maximum enhancement among all three luminescence components and dominates the whole EL spectra after decorated with Ag NPs and SiO_2 layer (Figure 5b). This phenomenon is consistent

DOI: 10.1021/acsami.5b08382
ACS Appl. Mater. Interfaces 2016, 8, 1653−1660

with the previous reports on LSP-enhanced n-ZnO/p-GaN heterojunction LEDs.[8,11−13]

However, by carefully comparing the improvements of PL and EL, one can find that there are some inconsistencies between them. First, the optimized spacer-layer thickness for EL is 12 nm, smaller than 16 nm for PL. Second, the maximum enhancement ratio in EL is 7-fold, "abnormally" higher than 3.5-fold observed in PL. Here, we tentatively give out the possible reasons for the two inconsistencies. For the difference in optimal spacer-layer thickness, the relatively larger thickness of 16 nm derived from PL measurements is thick enough to block the undesired charge transfer and nonradiative FRET between ZnO and Ag. However, as mentioned in the beginning, it also limits the carrier injection rate under external bias in EL characterizations. Thus, to achieve the best EL enhancement, the thickness of dielectric silica layer ought to be slightly reduced, which not only keeps the unwished charge transfer and nonradiative FRET being blocked, but also increases the carrier injection rate in some extent. So, the relatively thinner 12 nm SiO_2 spacer-layer presents the maximal EL improvement. On the other hand, the enhancement ratio observed from EL is usually the same as or slightly lower than that from PL, because of the more serious heating effect induced by injection current during EL measurements. Surprisingly, the experimental results are just the opposite: the enhancement ratio of EL is nearly twice that of PL. The exact mechanism for this "abnormal" phenomenon needs further investigation and should be related to the improved LEE from Ag NPs decorated waveguide-type NRA LED. This issue will be discussed in the following section in detail.

Many studies have proved that a nanorod with suitable dimensions can act as an optical waveguide.[34−37] To clearly illustrate this viewpoint, numerical simulations of light-wave electrical field intensity distribution in bare ZnO nanorod and Ag NPs decorated core/shell nanorod have been conducted and the results are shown in Figure 6a. Herein, FDTD solution 8.6 was chosen as the simulation toolkit. A dipole point light source (set as a transverse electric wave at wavelength of 380 nm) was placed at the interface between ZnO nanorod and p-GaN layer, corresponding to the heterojunction active region for exciton/electron−hole pair recombination. The results clearly show that the light is well confined within the ZnO nanorod, propagates along its axial direction, and finally emits from the nanorod's top surface (Figure 6a, left). Note that the refractive indices of SiO_2 and ZnO at 380 nm are 1.47 and 2.45, respectively,[38,39] indicating that the ZnO/SiO_2 core/shell nanorod itself is also a good optical waveguide. Such an optical confinement system will limit the LEE of NRA LED because the generated EL will be strongly self-absorbed during the upward propagation process. However, after spin-coating Ag NPs onto the core/shell nanorod, the light field energy will be coupled out of the nanorod optical waveguide during its propagation (Figure 6a, right). That is, the LEE, especially the lateral LEE of core/shell NRA LED, is notably improved as a result of resonant coupling between Ag LSPs and ZnO photons. Combined with the enhancement ratios of IQE (3.5-fold) and entire EL intensity (7-fold), the LEE improvement in EL is estimated to be 2-fold, which is consistent with the previous reports on ZnO- and GaN-based LEDs claiming that the LSP resonant effect can induce a 2- to 4-fold LEE improvement.[15,32,40] In a word, the EL enhancement is induced by the joint contributions of IQE improvement (exciton-LSP coupling near the active region) and LEE improvement (photon-LSP coupling during the EL propagation), as illustrated in Figure 6b. On the contrary, the PL enhancement is mainly dominated by the IQE improvement, as discussed before, while the LEE improvement effect is relatively weak in PL characterization. This is because the photoexcited excitons are mainly distributed in the near-surface region of ZnO nanorod top (usually several tens of nanometers; Figure 6c).[41,42] In this case, the exciton-LSP coupling is the primary near-field interaction mechanism leading to the IQE improvement. The spontaneous radiations directly enter into free space before the photon-LSP coupling can play an efficient role. Therefore, compared to the EL with dual improvement routes, the single route of IQE improvement aroused by exciton-LSP coupling in PL exhibits a relatively low overall enhancement ratio of 3.5-fold.

4. CONCLUSIONS

In summary, we have demonstrated the prototype devices of LSP-enhanced LEDs by introducing Ag NPs into ZnO/SiO_2 core/shell NRA/p-GaN heterostructures. Different from previous works, the thickness of SiO_2 spacer-layer employed here was carefully optimized via actual EL characterizations. By comparatively studying the PL and EL spectra of these LEDs, we note that the enhancement ratios deduced from EL and PL measurements show different shell thickness dependences. On the basis of the analyses of TR-PL characterization, theoretical estimation, and FDTD simulation, two sets of enhancement mechanism, including the joint improvement of IQE and LEE in EL and single improvement of IQE in PL, were proposed to explain the observed "freaky" phenomena. For the actual LED device working under external voltage, both the SiO_2 shell thickness of 12 nm and 7-fold luminescence enhancement determined through EL characterizations are the really optimized and needed results in the current study. Actually, the higher enhancement ratio obtained in EL is more meaningful in practical applications and the present work provides a feasible way to improve both the IQE and LEE of current LEDs.

■ ASSOCIATED CONTENT

Supporting Information

The Supporting Information is available free of charge on the ACS Publications website at DOI: 10.1021/acsami.5b08382.

Schematic flowcharts for the preparation of ZnO/SiO_2 core/shell NRAs and XRD patterns of these ZnO/SiO_2 core/shell NRAs with and without Ag NPs decoration. (PDF)

■ AUTHOR INFORMATION

Corresponding Authors

*E-mail: hyxu@nenu.edu.cn.
*E-mail: ycliu@nenu.edu.cn.

Notes

The authors declare no competing financial interest.

■ ACKNOWLEDGMENTS

This work is supported by the NSFC for Excellent Young Scholars (No. 51422201), the Program of NSFC (No. 51172041, 51372035, 91233204 and 61505026), 973 Program (No. 2012CB933703), "111" Project (No. B13013), Research Fund for the Doctoral Program of Higher Education (No. 20130043110004), the 2015 Open Project from State Key

DOI: 10.1021/acsami.5b08382
ACS Appl. Mater. Interfaces 2016, 8, 1653−1660

Laboratory of Applied Optics (No. 202115002), the Open Project from Key Laboratory for UV-Emitting Materials and Technology of Ministry of Education (No. 130014548), the China Postdoctoral Science Foundation funded project (No. 2015M580238) and the Fundamental Research Funds for the Central Universities (No. 2412015BJ003 and 2412015KJ008).

REFERENCES

(1) Zhu, H.; Shan, C.-X.; Yao, B.; Li, B.-H.; Zhang, J.-Y.; Zhang, Z.-Z.; Zhao, D.-X.; Shen, D.-Z.; Fan, X.-W.; Lu, Y.-M.; Tang, Z.-K. Ultralow-Threshold Laser Realized in Zinc Oxide. *Adv. Mater.* **2009**, *21*, 1613−1617.

(2) Dai, J.; Xu, C. X.; Sun, X. W. ZnO-Microrod/P-GaN Heterostructured Whispering-Gallery-Mode Microlaser Diodes. *Adv. Mater.* **2011**, *23*, 4115−4119.

(3) Chu, S.; Wang, G.; Zhou, W.; Lin, Y.; Chernyak, L.; Zhao, J.; Kong, J.; Li, L.; Ren, J.; Liu, J. Electrically Pumped Waveguide Lasing from ZnO Nanowires. *Nat. Nanotechnol.* **2011**, *6*, 506−510.

(4) Zhang, X.-M.; Lu, M.-Y.; Zhang, Y.; Chen, L.-J.; Wang, Z. L. Fabrication of A High-Brightness Blue-Light-Emitting Diode Using A ZnO-Nanowire Array Grown on P-GaN Thin Film. *Adv. Mater.* **2009**, *21*, 2767−2770.

(5) Liu, W. Z.; Xu, H. Y.; Ma, J. G.; Liu, C. Y.; Liu, Y. X.; Liu, Y. C. Effect of Oxygen-Related Surface Adsorption on The Efficiency and Stability of ZnO Nanorod Array Ultraviolet Light-Emitting Diodes. *Appl. Phys. Lett.* **2012**, *100*, 203101.

(6) Zhang, C.; Marvinney, C. E.; Xu, H. Y.; Liu, W. Z.; Wang, C. L.; Zhang, L. X.; Wang, J. N.; Ma, J. G.; Liu, Y. C. Enhanced Waveguide-Type Ultraviolet Electroluminescence from ZnO/MgZnO Core/Shell Nanorod Array Light-Emitting Diodes via Coupling with Ag Nanoparticles Localized Surface Plasmons. *Nanoscale* **2015**, *7*, 1073−1080.

(7) Ni, P. N.; Shan, C. X.; Li, B. H.; Wang, S. P.; Shen, D. Z. Bias-Polarity Dependent Ultraviolet/Visible Switchable Light-Emitting Devices. *ACS Appl. Mater. Interfaces* **2014**, *6*, 8257−8262.

(8) Liu, W. Z.; Xu, H. Y.; Zhang, L. X.; Zhang, C.; Ma, J. G.; Wang, J. N.; Liu, Y. C. Localized Surface Plasmon-Enhanced Ultraviolet Electroluminescence from N-ZnO/I-ZnO/P-GaN Heterojunction Light-Emitting Diodes via Optimizing The Thickness of MgO Spacer Layer. *Appl. Phys. Lett.* **2012**, *101*, 142101.

(9) Okamoto, K.; Niki, I.; Shvartser, A.; Narukawa, Y.; Mukai, T.; Scherer, A. Surface-Plasmon-Enhanced Light Emitters Based on InGaN Quantum Wells. *Nat. Mater.* **2004**, *3*, 601−605.

(10) Gu, X.; Qiu, T.; Zhang, W.; Chu, P. K. Light-Emitting Diodes Enhanced by Localized Surface Plasmon Resonance. *Nanoscale Res. Lett.* **2011**, *6*, 199−210.

(11) Zhang, S. G.; Zhang, X. W.; Yin, Z. G.; Wang, J. X.; Dong, J. J.; Gao, H. L.; Si, F. T.; Sun, S. S.; Tao, Y. Localized Surface Plasmon-Enhanced Electroluminescence from ZnO-Based Heterojunction Light-Emitting Diodes. *Appl. Phys. Lett.* **2011**, *99*, 181116.

(12) Qiao, Q.; Shan, C.-X.; Zheng, J.; Li, B.-H.; Zhang, Z.-Z.; Zhang, L.-G.; Shen, D.-Z. Localized Surface Plasmon Enhanced Light-Emitting Devices. *J. Mater. Chem.* **2012**, *22*, 9481−9484.

(13) Liu, W. Z.; Xu, H. Y.; Wang, C. L.; Zhang, L. X.; Zhang, C.; Sun, S. Y.; Ma, J. G.; Zhang, X. T.; Wang, J. N.; Liu, Y. C. Enhanced Ultraviolet Emission and Improved Spatial Distribution Uniformity of ZnO Nanorod Array Light-Emitting Diodes via Ag Nanoparticles Decoration. *Nanoscale* **2013**, *5*, 8634−8639.

(14) Lu, J.; Li, J.; Xu, C.; Li, Y.; Dai, J.; Wang, Y.; Lin, Y.; Wang, S. Direct Resonant Coupling of Al Surface Plasmon for Ultraviolet Photoluminescence Enhancement of ZnO Microrods. *ACS Appl. Mater. Interfaces* **2014**, *6*, 18301−18305.

(15) Zhang, C.; Xu, H. Y.; Liu, W. Z.; Yang, L.; Zhang, J.; Zhang, L. X.; Wang, J. N.; Ma, J. G.; Liu, Y. C. Enhanced Ultraviolet Emission from Au/Ag-Nanoparticles@MgO/ZnO Heterostructure Light-Emitting Diodes: A Combined Effect of Exciton- and Photon- Localized Surface Plasmon Couplings. *Opt. Express* **2015**, *23*, 15565−15574.

(16) Li, J.; Xu, C.; Nan, H.; Jiang, M.; Gao, G.; Lin, Y.; Dai, J.; Zhu, G.; Ni, Z.; Wang, S.; Li, Y. Graphene Surface Plasmon Induced Optical Field Confinement and Lasing Enhancement in ZnO Whispering-Gallery Microcavity. *ACS Appl. Mater. Interfaces* **2014**, *6*, 10469−10475.

(17) Lu, J.; Xu, C.; Dai, J.; Li, J.; Wang, Y.; Lin, Y.; Li, P. Improved UV Photoresponse of ZnO Nanorod Arrays by Resonant Coupling with Surface Plasmons of Al Nanoparticles. *Nanoscale* **2015**, *7*, 3396−3403.

(18) Atwater, H. A.; Polman, A. Plasmonics for Improved Photovoltaic Devices. *Nat. Mater.* **2010**, *9*, 205−213.

(19) Ni, W. H.; An, J.; Lai, C. W.; Ong, H. C.; Xu, J. B. Emission Enhancement from Metallodielectric-Capped ZnO Films. *J. Appl. Phys.* **2006**, *100*, 026103.

(20) Lawrie, B. J.; Haglund, R. F., Jr.; Mu, R. Enhancement of ZnO Photoluminescence by Localized and Propagating Surface Plasmons. *Opt. Express* **2009**, *17*, 2565−2572.

(21) Shen, K.-C.; Liao, C.-H.; Yu, Z.-Y.; Wang, J.-Y.; Lin, C.-H.; Kiang, Y.-W.; Yang, C. C. Effects of The Intermediate SiO_2 Layer on Polarized Output of A Light-Emitting Diode with Surface Plasmon Coupling. *J. Appl. Phys.* **2010**, *108*, 113101.

(22) Haglund, R. F., Jr.; Lawrie, B. J.; Mu, R. Coupling of Photoluminescent Centers in ZnO to Localized and Propagating Surface Plasmons. *Thin Solid Films* **2010**, *518*, 4637−4643.

(23) Zhang, D.; Ushita, H.; Wang, P.; Park, C.; Murakami, R.-i.; Yang, S.-c.; Song, X. Photoluminescence Modulation of ZnO via Coupling with The Surface Plasmon Resonance of Gold Nanoparticles. *Appl. Phys. Lett.* **2013**, *103*, 093114.

(24) Mahanti, M.; Basak, D. Enhanced Photoluminescence in Ag@SiO_2 Core-Shell Nanoparticles Coated ZnO Nanorods. *J. Lumin.* **2014**, *154*, 535−540.

(25) Mahanti, M.; Basak, D. Enhanced Emission Properties of Au/SiO_2/ZnO Nanorod Layered Structure: Effect of SiO_2 Spacer Layer and Role of Interfacial Charge Transfer. *RSC Adv.* **2014**, *4*, 15466−15473.

(26) Liu, W.; Liang, Y.; Xu, H.; Wang, L.; Zhang, X.; Liu, Y.; Hark, S. Heteroepitaxial Growth and Spatially Resolved Cathodoluminescence of ZnO/MgZnO Coaxial Nanorod Arrays. *J. Phys. Chem. C* **2010**, *114*, 16148−16152.

(27) Wang, L.; Zhang, X.; Fu, Y.; Li, B.; Liu, Y. Bioinspired Preparation of Ultrathin SiO_2 Shell on ZnO Nanowire Array for Ultraviolet-Durable Superhydrophobicity. *Langmuir* **2009**, *25*, 13619−13624.

(28) Wang, L.; Zhang, X.; Li, B.; Sun, P.; Yang, J.; Xu, H.; Liu, Y. Superhydrophobic and Ultraviolet-Blocking Cotton Textiles. *ACS Appl. Mater. Interfaces* **2011**, *3*, 1277−1281.

(29) Maier, S. A.; Atwater, H. A. Plasmonics: Localization and Guiding of Electromagnetic Energy in Metal/Dielectric Structures. *J. Appl. Phys.* **2005**, *98*, 011101.

(30) Liu, W. Z.; Xu, H. Y.; Wang, L.; Li, X. H.; Liu, Y. C. Size-Controlled Growth of ZnO Nanowires by Catalyst-Free High-Pressure Pulsed Laser Deposition and Their Optical Properties. *AIP Adv.* **2011**, *1*, 022145.

(31) Liu, K. W.; Tang, Y. D.; Cong, C. X.; Sum, T. C.; Huan, A. C. H.; Shen, Z. X.; Wang, L.; Jiang, F. Y.; Sun, X. W.; Sun, H. D. Giant Enhancement of Top Emission from ZnO Thin Film by Nano-patterned Pt. *Appl. Phys. Lett.* **2009**, *94*, 151102.

(32) Yang, W.; Xie, Y.; Liao, R.; Sun, J.; Wu, Z.; Wong, L.; Wang, S.; Wang, C.; Lee, A.; Gong, H. Enhancement of Bandgap Emission of Pt-Capped MgZnO Films: Important Role of Light Extraction versus Exciton-Plasmon Coupling. *Opt. Express* **2012**, *20*, 14556−14563.

(33) Dai, J.; Ji, Y.; Xu, C. X.; Sun, X. W.; Leck, K. S.; Ju, Z. G. White Light Emission from CdTe Quantum Dots Decorated N-ZnO Nanorods/P-GaN Light-Emitting Diodes. *Appl. Phys. Lett.* **2011**, *99*, 063112.

(34) Li, W.; Gao, M.; Cheng, R.; Zhang, X.; Xie, S.; Peng, L.-M. Angular Dependent Luminescence of Individual Suspended ZnO Nanorods. *Appl. Phys. Lett.* **2008**, *93*, 023117.

DOI: 10.1021/acsami.5b08382
ACS Appl. Mater. Interfaces 2016, 8, 1653−1660

(35) Lai, E.; Kim, W.; Yang, P. Vertical Nanowire Array-Based Light Emitting Diodes. *Nano Res.* **2008**, *1*, 123−128.
(36) Zimmler, M. A.; Bao, J.; Capasso, F.; Müller, S.; Ronning, C. Laser Action in Nanowires: Observation of The Transition from Amplified Spontaneous Emission to Laser Oscillation. *Appl. Phys. Lett.* **2008**, *93*, 051101.
(37) Fu, H.-K.; Cheng, C.-L.; Wang, C.-H.; Lin, T.-Y.; Chen, Y.-F. Selective Angle Electroluminescence of Light-Emitting Diodes Based on Nanostructured ZnO/GaN Heterojunctions. *Adv. Funct. Mater.* **2009**, *19*, 3471−3475.
(38) Xu, S.; Xu, C.; Liu, Y.; Hu, Y.; Yang, R.; Yang, Q.; Ryou, J. H.; Kim, H. J.; Lochner, Z.; Choi, S.; Dupuis, R.; Wang, Z. L. Ordered Nanowire Array Blue/Near-UV Light Emitting Diodes. *Adv. Mater.* **2010**, *22*, 4749−4753.
(39) Zhu, H.; Shan, C. X.; Wang, L. K.; Yang, Y.; Zhang, J. Y.; Yao, B.; Shen, D. Z.; Fan, X. W. A Route to Improved Extraction Efficiency of Light-Emitting Diodes. *Appl. Phys. Lett.* **2010**, *96*, 041110.
(40) Homeyer, E.; Mattila, P.; Oksanen, J.; Sadi, T.; Nykänen, H.; Suihkonen, S.; Symonds, C.; Tulkki, J.; Tuomisto, F.; Sopanen, M.; Bellessa, J. Enhanced Light Extraction from InGaN/GaN Quantum Wells with Silver Gratings. *Appl. Phys. Lett.* **2013**, *102*, 081110.
(41) He, T. C.; Chen, R.; Lin, W. W.; Huang, F.; Sun, H. D. Two-Photon-Pumped Stimulated Emission from ZnO Single Crystal. *Appl. Phys. Lett.* **2011**, *99*, 081902.
(42) Foreman, J. V.; Everitt, H. O.; Yang, J.; McNicholas, T.; Liu, J. Effects of Reabsorption and Spatial Trap Distributions on The Radiative Quantum Efficiencies of ZnO. *Phys. Rev. B: Condens. Matter Mater. Phys.* **2010**, *81*, 115318.

DOI: 10.1021/acsami.5b08382
ACS Appl. Mater. Interfaces 2016, 8, 1653−1660